Coulomb explosion in ultrashort pulsed laser ablation of Al_2O_3

R. Stoian,* D. Ashkenasi, A. Rosenfeld, and E. E. B. Campbell[1,†]
Max-Born Institut für Nichtlineare Optik und Kurzzeitspektroscopie, Rudower Chaussee 6, D-12489 Berlin, Germany
[1]*School of Physics and Engineering Physics, Gothenburg University & Chalmers University of Technology, S-41296 Gothenburg, Sweden*
(Received 22 February 2000)

Coulomb explosion (CE) is identified as the mechanism of ion ejection under low fluence ultrashort pulse laser ablation of crystalline Al_2O_3. The ion momenta are equal during ''gentle'' ablation. This is explained by impulsive CE from the surface region lasting ~1 ps. The onset of ''strong'' ablation leads to a decrease in the measured ion velocities. The kinetic energies rather than the momenta of the ions become equal. This regime is associated with strong plasma light emission and crater formation.

I. INTRODUCTION

There is growing interest in the comparison between material modifications induced by ultrashort pulsed lasers and energetic ion beams.[1] This is partly due to the increasing availability of relatively compact, intense, ultrashort pulse laser systems that can be used to couple large amounts of energy into the target on a femtosecond time scale, comparable to the situation with energetic ion bombardment. The secondary effects that concealed much of the fundamental physical processes occurring for laser ablation with standard nanosecond pulsed lasers such as laser heating of the ablated material[2] can be avoided with ultrashort pulses. This is beginning to open the way to a more detailed understanding of the laser-material interactions and mechanisms of material removal.[3]

One phenomenon that has recently been the subject of considerable interest is that of sputtering due to highly-charged-ion impact on surfaces.[4–9] Experimental evidence is accumulating that this may have technological significance for modifying or etching semiconductor or insulator surfaces on a nanometer scale.[5,10–12] The use of highly charged ions is attractive due to the possibility of obtaining high sputter yields at low impact energies and without inducing radiation defects in deeper layers of the material. However, there is very little information about the Coulomb-explosion process that has been proposed to be the main cause of surface damage and material removal[5,8] and, indeed, this interpretation is sometimes regarded as being questionable.[9] The main experimental result used to justify an explanation in terms of Coulomb explosion is an increase in secondary-ion emission and a charge-state-dependent kinetic energy observed in collisions with very highly charged ions with charge up to $70+$.[5] Recent molecular dynamics (MD) simulations of Coulomb explosions on silicon surfaces have shown that this mechanism can lead to the production of nanometer scale structures on the surface that are at least in qualitative agreement with what is seen experimentally in highly-charged-ion–surface collisions ($q>40+$, typically).[6] The results of these simulations show many similarities with the results of simulations of ultrashort pulse laser ablation of silicon for femtosecond pulse durations.[13,14] Both calculations showed an initial fast, explosive (100 fs–1 ps) removal of positive ions due to Coulomb repulsion from the surface followed by relaxation of the target and ballistic and thermal removal of neutral particles on the picosecond time scale. It should, however, be mentioned that the MD simulations employ relatively simple phenomenological potentials and are certainly not able to accurately treat the dynamics of the electronically excited states. They should thus be regarded as a qualitative indication of the dynamical effects that might be expected to occur in both highly-charged-ion and ultrashort pulse laser sputtering. It would thus appear that ultrashort pulse laser ablation studies may provide an accessible means of obtaining detailed information on the mechanisms leading to particle emission and could be an important addition to the experimental methods presently applied to explore the role of Coulomb explosion in the nanostructuring of insulator and semiconductor surfaces.

In this paper we report strong experimental indications for the occurrence of a macroscopic Coulomb explosion from a highly charged surface (Al_2O_3). This should be distinguished from the submonolayer laser-induced desorption of atoms or ions from excited two-hole states as, e.g., observed recently from Si (Ref. 15) where atoms are desorbed with a characteristic kinetic energy (in this case 0.06 eV) from an electronically repulsive state at the surface. Such processes are generally site specific and related to the specific bonding properties of different adatom sites.[16] The macroscopic Coulomb explosion reported here, with the removal of many monolayers per laser shot, leads to much higher kinetic energies on the order of 100 eV with equal momenta for ions of different mass, as would be expected from an impulsive acceleration from a surface with high charge density. It is clearly observable under low-laser-fluence conditions that lead to macroscopic ablation but are not sufficient to induce the formation of a dense plasma, as indicated by the low intensity of light observed (mainly scattering from the surface). When strong plasma emission is observed optically it is accompanied by the appearance of an intense low-velocity component in the ion-velocity distributions. For conditions where strong ablation and dense plasma formation are dominant, the kinetic energies of the different ion species tend to be equal, indicating their origin in the decay of the plasma plume.

II. EXPERIMENTAL SETUP

A Ti:sapphire oscillator-amplifier laser system based on the chirped-pulse-amplification (CPA) technique and producing light of wavelength 800 nm with a pulse duration of 0.1 ps (unless otherwise stated) was used in the experiments. The laser beam was focused onto the sample surface, giving a focus area (at $1/e^2$) of $\sim 470\ \mu m^2$. For the experiments reported here, the laser fluence at the sample surface was 5 and 4 J/cm^2 for 0.1 and 0.2-ps pulses, respectively, slightly above the single-shot ablation threshold. The single-crystalline samples were polished and supported on a metal target holder such that the laser processed area was not backed. The ablation was carried out under vacuum conditions (10^{-3} Pa).

Positively charged Al^+ and O^+ ions were detected by a linear time-of-flight (TOF) mass spectrometer based on the Wiley-McLaren configuration.[17] The ions were allowed to drift for 65 mm and then extracted into the mass spectrometer with a variable delay pulsed electric field and detected with a microsphere plate (MSP). The extraction grids of the mass spectrometer were either arranged parallel to the substrate surface with a 25° angle of incidence of the laser beam (with respect to the surface normal) or vice versa (normal incidence of the laser beam with the grids at an angle of 25°). The delayed pulsed extraction allows the determination of the mass-resolved velocity distribution of the ions. No molecular or cluster ions were detected in the experiments.

III. RESULTS AND DISCUSSION

The ultrashort pulse laser ablation of Al_2O_3 has been the subject of a number of investigations.[17–21] One of the most characteristic features is the occurrence of two clearly distinguishable ablation regimes:[18–20] a ''gentle'' ablation in which a few nanometers in depth is removed per laser shot and that leaves behind a smooth surface and a ''strong'' ablation phase characterized by an order of magnitude higher ablation rate per pulse and showing characteristics of ''phase explosion.'' These characteristics are quite different from the ablation behavior under irradiation with the more standard nanosecond UV laser pulses.[22] For a detailed discussion see Ashkenasi *et al.*[18] and references given therein. For the conditions used in the present experiments (100 fs, 800 nm, 5 J cm^{-2}) the initial ablation corresponds to the ''gentle'' phase. After a certain number of laser shots the underlying material has accumulated a sufficiently high density of defects to initiate the ''strong'' ablation phase (see below). The crossover occurs after approximately 20 laser shots. This can be seen in Fig. 1, where scanning electron microscope pictures of the surface after irradiation with a given number of laser shots are shown.

Velocity distributions for Al^+ and O^+ are shown in Fig. 2, for normal laser incidence (25° TOF-axis incidence), as a function of number of laser shots. It is immediately apparent that the most probable velocity of both species decreases as the number of laser shots increases due to the strong onset of a low-velocity component in the distribution. (Note that the data have been normalized to the individual maximum intensity.) This is, at first sight, counter intuitive since there is approximately an order of magnitude more material removed per shot in the strong phase compared to the gentle phase[18] and the surface morphology shows more evidence of a ''violent'' material removal (Fig. 1). The data can be reasonably well fitted by single Maxwell-Boltzmann (MB) distributions when ablation is clearly either within the gentle phase ($N=4$) or the strong phase ($N=100$). For these comparisons we have used one-dimensional (1D) MB fitting functions ($I(v) \propto \exp[-m(v-u)^2/2kT]$, with m the mass of the ions and u the flow velocity). We do not want to infer that this is the best fit function to be used for our experiments but it does seem to be the most appropriate, simple, compromising choice for our experimental conditions. The best fits for the Al^+ data are shown in Fig. 2. The $N=4$ distribution has a flow velocity of $u=(2.1\pm0.1)\times10^4$ m s^{-1} and a translational temperature, $kT=13\pm1$ eV. The $N=100$ data are fitted with a flow velocity $u=10^4$ m s^{-1} and a translational temperature of 5 eV. It is more difficult to satisfactorily fit the intermediate distributions ($N=50$ and 70). The fits shown in the figure are the sums of two MB distributions: a slow distribution with $u=1.4\times10^4$ m s^{-1} ($kT=8$ eV) and a fast distribution that is the same as that for $N=4$ but with decreasing relative intensity as N increases. The calculated distributions shown for O^+ have the same translational temperatures as those fitted to the Al^+ data, but the flow velocities have been scaled to give the same value for the momentum, as discussed below. The comparison of the Al^+ fit parameters with the O^+ data is reasonably good for up to $N=70$ but becomes much worse after this using the momentum scaling (not shown on Fig. 2 due to low intensities and poor signal-to-noise ratio for this particular set of data).

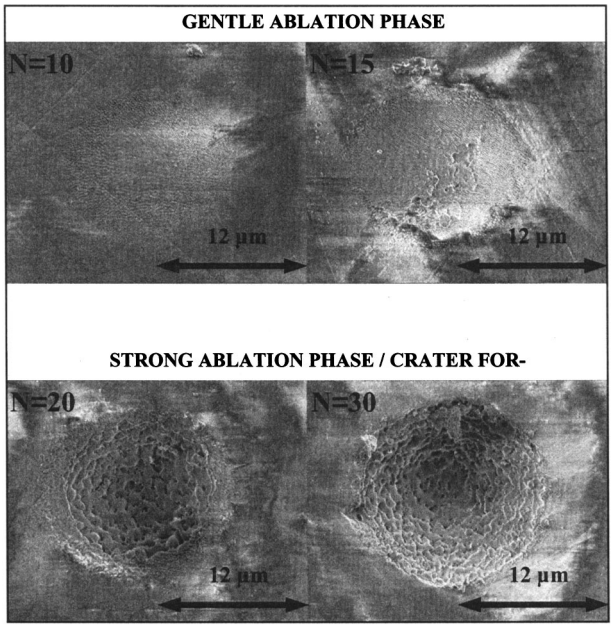

FIG. 1. Scanning electron microscopy pictures of the irradiated spot at different number of pulses per site. One can clearly see the change from gentle to strong ablation as N increases.

The maxima of the measured velocity distributions, which are equivalent to the drift velocities u from the 1D MB fits, have been plotted in Fig. 3 as both momenta [Fig. 3(a)] and kinetic energies [Fig. 3(b)] as a function of N. The values given for O^+ were obtained from separately fitting the experimental data (as discussed for Al^+, above) and not taken from the scaled fits shown in Fig. 2. This very clearly shows that the momenta of the two ablated species are equal for low

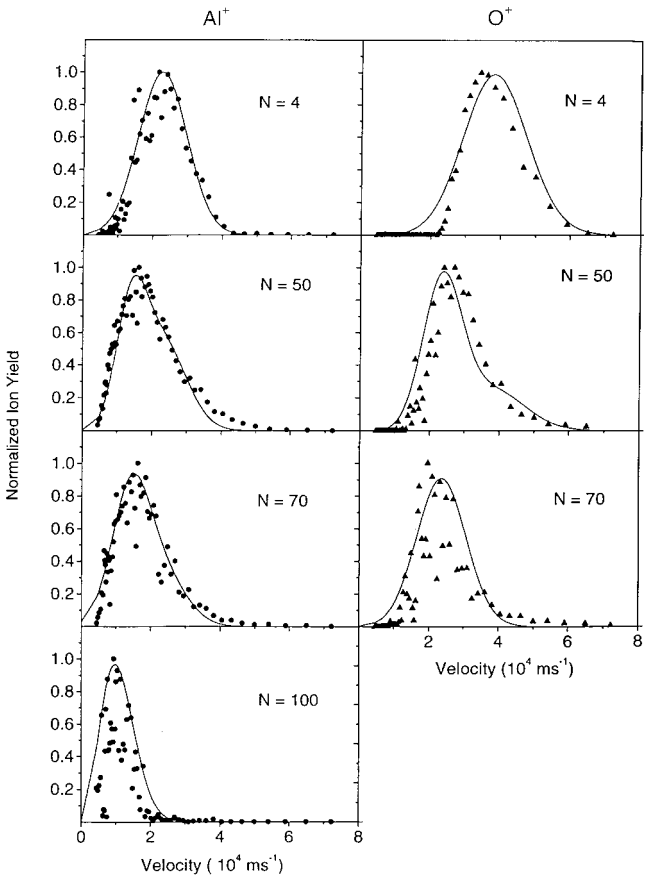

FIG. 2. Velocity distributions for O^+ and Al^+ ions for different numbers of laser shots per site. Left-hand side. Al^+ (circles), right-hand side: O^+ (triangles). The Al^+ data are fitted by 1D Maxwell-Boltzmann distributions (full lines). The solid lines on the O^+ plots are the same distributions scaled according to the mass. See text for details.

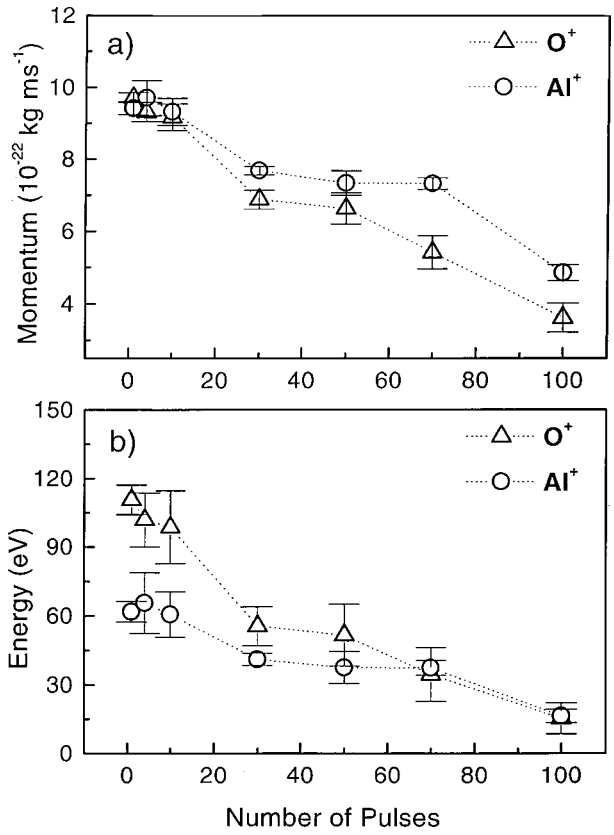

FIG. 3. (a) Momentum and (b) energy of O^+ and Al^+ species within the plume as a function of number of laser shots. The values were calculated from the measured maxima in the velocity distributions. Circles, Al^+; triangles, O^+.

number of laser shots, i.e., when ablation is ''gentle.'' There is an intermediate range ($\sim 20 \leqslant N \leqslant 70$) where the most probable velocity corresponds to neither the same momentum nor the same energy. Finally for $N \geqslant 70$, where ablation is well within the strong regime, accompanied by plasma light emission and crater formation, the ions clearly have the same kinetic energies. The flow velocity u used for the fit of the fast distribution ($N=4$) in Fig. 2 corresponds in both cases (Al^+ and O^+) to the momentum shown in Fig. 3, i.e., $9.5\times 10^{-22} m_{\mathrm{Al/O}}$. Very similar behavior is observed for 25° laser incidence (ion extraction with grids parallel to the surface). The only difference is an increase in the detected drift velocity of the fast ions when using the arrangement with ion extraction grids parallel to the surface. This is discussed in more detail elsewhere.[23]

The correlation between plasma light emission, strong ablation, and the presence of a low-velocity component in the ion distributions is further illustrated by Fig. 4. Here the light scattering or emission is detected by a charge-coupled device (CCD) camera. For low numbers of laser shots, i.e., when the ablation is still in the gentle phase, we only detected a small amount of light scattered from the substrate surface. As soon as the crossover to the strong ablation phase occurs (for $N > 30$ in this case), as characterized by an increase in the amount of material removed per pulse and the appearance of low-velocity ions, a strong light emission is detected from the plasma plume.

Ions of the same momenta, as clearly seen during the gentle ablation phase, would be expected from an impulsive Coulomb explosion from a highly charged surface. The intense laser pulse will induce strong ionization from the surface and underlying regions. The emission of electrons from the surface will leave a high concentration of uncompensated positive charge. The amount of uncompensated charge will

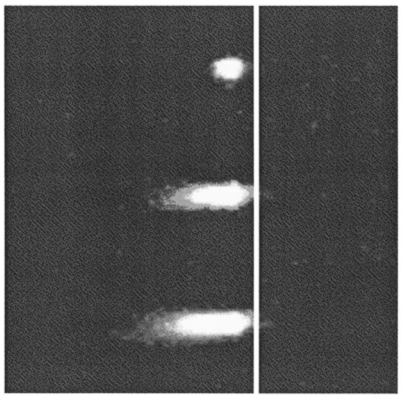

FIG. 4. Light emission/scattering from the irradiated surface detected by a CCD camera. $N=6$, gentle ablation; only scattered light from the surface is detected. For $N=35$ and 48 strong ablation is present and there is clearly plasma light emission from the ablated plume. The laser pulse duration was 0.2 ps.

be neutralized either by charge losses in the process of ion ejection or, less likely for dielectrics, electron supply from the bulk or hole diffusion from the irradiated region or by recombination with slow electrons returning to the surface.[24] The neutralization process is not instantaneous due to the electrical properties of Al_2O_3. The repulsive electric field induced by the laser pulse lasts for a short period of time and the Al^+ and O^+ spend basically the same time in the action range of this field. The strength of the electrostatic field is determined by the charge density, which is controlled by the flux of the emitted ions. The electrostatic interaction leading to the ion removal is thus many orders of magnitude shorter than the ion flight time to the mass spectrometer, and considerations of the conservation of momentum will lead to equal momenta for the ejected Al^+ and O^+ ions as seen experimentally. This can be described by the expression, $p = F_{el}\tau$, where p is the momentum for the two species in the plume, F_{el} is the electric force at the surface due to charge accumulation, and τ is the time spent by the particles in the action range of this field ($\sim$1 ps).

One can estimate the minimum charge density at the surface to induce a Coulomb explosion. The electrostatic stress (force per unit area) has to overcome the local mechanical (or bonding) stress.[25] For the bulk material this can be estimated by $E/10$ where E is the Young's modulus of the material.[26] For atoms in the surface layer this will obviously be considerably smaller. We take a compromise average value of $E/20$ for our estimates and obtain

$$f > \left(\frac{\pi^2 \epsilon a_0^4 E}{20 l e^2} \right)^{1/2},$$

where f is the average fractional degree of ionization per atom, ϵ is the bulk dielectric constant ($10\epsilon_0$), a_0 is the average interatomic spacing in the lattice (2 Å) and l is a factor taking into account the lattice geometry (3.64). For Al_2O_3 we obtain $f > 0.5$ (with an estimated error of $\sim$50%). Similarly, we can estimate the fractional charge needed to produce the observed momentum of $9.5 \times 10^{-22}\,\mathrm{kg\,m\,s^{-1}}$ (Fig. 3). Assuming that the force acts for 1 ps we obtain the very reasonable value of $f = 0.65$. The observed momenta and therefore also the ion kinetic energies are thus consistent with an average surface ionization of 65%. The observed momenta are slightly fluence dependent very close to threshold, increasing as the fluence is increased. However, they rather rapidly converge to the values presented here. An additional check on the order of magnitude estimate given here can be obtained from considering the field applied by a homogeneously charged sheet. If we assume an average surface ionization of 65%, as obtained from the analysis above, and calculate the field from an infinitely plane conductor using $S/(2\varepsilon)$ where S is the charge surface density ($\sim$2.2 C/m^2) and ε is the electrical permittivity, we obtain a momentum for the repelled ions of $2 \times 10^{-21}\,\mathrm{kg\,m\,s^{-1}}$. This is only a factor of 2 larger than that observed in our experiments and further supports the interpretation in terms of Coulomb explosion.

The overall degree of ionization in our ablated material during the gentle phase can be estimated from the volume of the produced crater and the ion intensities (integrated over velocity and angle and corrected for detection efficiency and amplification) to be slightly more than 10%. This is considerably less than the 65% estimated above; however, this is exactly what one would expect from considering the results of the molecular dynamics simulations.[6,13,14] They showed that the ions are removed from a shallow surface region with the bulk of the material removal occurring later as slower neutral species after relaxation and heating of the lattice. Our results, where we are removing $\sim$25 nm per pulse in the gentle phase, suggest that the ions are removed from a surface region with a depth of approximately 2–3 nm, corresponding to roughly four lattice parameters.

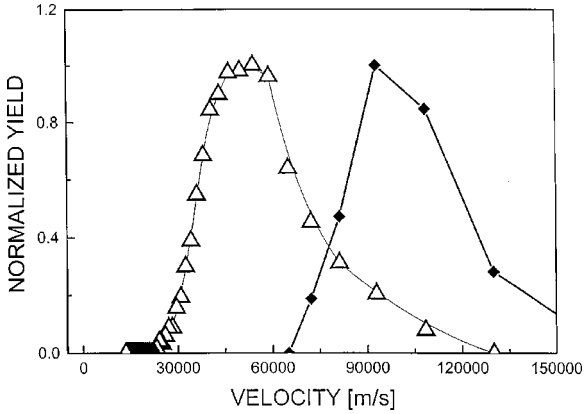

FIG. 5. Normalized velocity distributions for O^+ (open triangles) and O^{2+} (closed diamonds), showing that the doubly charged ions have twice the velocity of the singly charged ions. (TOF is normal to surface; $N = 2$; gentle ablation.)

We also observe a small amount of doubly charged ions, contributing 10–15 % of the total ion signal. The normalized velocity distributions for O^+ and O^{2+} are shown in Fig. 5 for ion extraction with grids parallel to the surface. The doubly charged ions have velocities that are twice as fast as the singly charged ions. This is a further confirmation of the charged-scaled momenta the ions obtain due to the impulsive Coulomb explosion from the surface.

The lack of very highly charged ions and the magnitude of the ion kinetic energies is different from what has been observed in experiments involving sputtering due to the impact of highly charged ions (as discussed in the Introduction).[5,6] This is a consequence of the much more homogeneous situation present in the laser experiments rather than a difference in the underlying mechanisms leading to material removal. There is a much more homogeneous charge distribution produced over the entire irradiated area in the laser experiments leading to the removal of the entire upper layers. In highly-charged-ion experiments the projectile ion strips many electrons from only a few atoms in its path, thus producing a very small region with an extremely high charge density initially surrounded by normal bulk material. This will presumably lead to the explosive removal of a few highly charged ions with correspondingly high kinetic energies.

With increasing number of laser shots, N, the behavior changes noticeably. After approximately 20 shots, for the conditions used here, the ablation is much more efficient with up to an order of magnitude more material being removed per pulse. The onset of this ablation phase is also accompanied by the emission of plasma light from the sur-

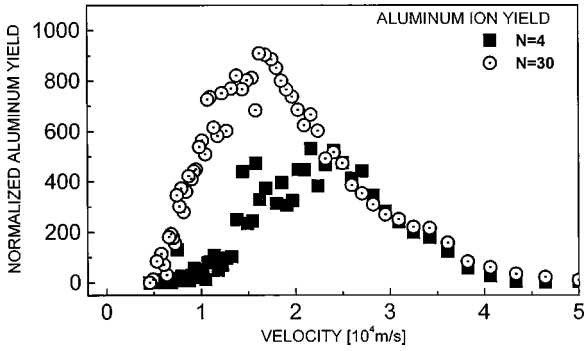

FIG. 6. Velocity distributions for Al^+ in the gentle (black squares) and strong (circles) ablation phases showing the absolute ion intensities. Fast ions are still present during the strong ablation but are masked by the strong thermal distribution (laser normal to surface).

face (Fig. 4) and characterized by a noticeable shift in the maxima of the velocity distributions of the ions towards lower values (Fig. 2). The fast Coulomb explosion ions are still present, as seen in Fig. 6 where the absolute intensities of Al^+ have been compared for velocity distributions measured during the gentle and strong ablation phases. However, they are vastly overshadowed by the slow ions in the strong ablation. There is a strong incubation behavior with previous laser pulses building up an increasing density of defect sites in the target below the ablated region.[3,27] Strong incubation effects have also been observed in experiments that study the dependence of the ablation threshold on the number of laser shots both specifically for Al_2O_3 (Ref. 28) and for other dielectric materials (Refs. 29 and 30). The increasing density of defects in the underlying material leads to a much more rapid ionization in the bulk due to lower-order absorption from defect sites and an extremely rapid heating of the lattice to a temperature close to the thermodynamic critical temperature. A recent study[30] has shown that the main cause of macroscopic laser damage in dielectrics is avalanche ionization. However, this requires a certain free-electron density to be initiated. With a gradual buildup of defect density with increasing number of laser shots it becomes increasingly easy, for the same laser fluence, to produce the necessary free-electron density for avalanche ionization (via multiphoton absorption from defect states) at an early stage of the ultrashort laser pulse. This therefore leads to a much more efficient coupling of energy into the substrate as the number of laser shots increases. In addition, the defect sites themselves will act as trapping sites and contribute to a more efficient energy coupling to the lattice. Dense plasma formation, accompanied by clearly observable light emission and an explosive removal of material in a mixture of vapor and liquid droplets, then occurs under these conditions.[3,18,19,31] We interpret the lower velocities and equal kinetic energies measured for $N=100$ to be due to ions from the gas-phase ionized vapor plume (from which light is also clearly emitted). These ''plasma ions'' would be expected to have the same kinetic energy or temperature. More work is needed to be certain about the origin of the ions under these conditions but some supporting results are available from preliminary measurements of the angular distributions of the ions.[23,32] The fast ions observed for low numbers of laser shots that we

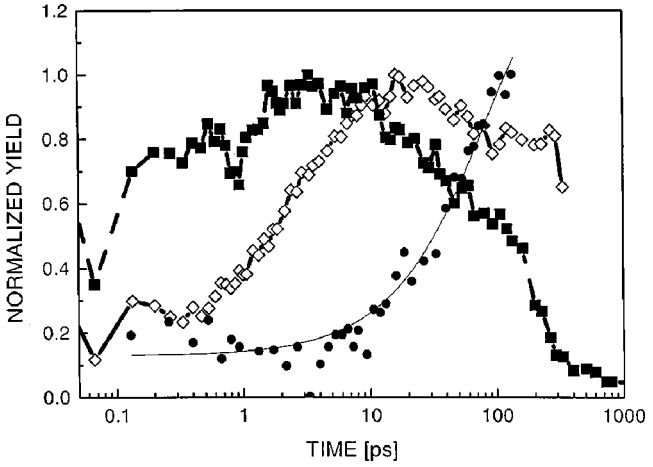

FIG. 7. Dependence of Al^+-ion intensity on the delay between two laser pulses of equal fluence. The individual pulse fluences are below the ablation threshold but the sum lies above (3.5 J/cm^2). Black squares: fast ions with a velocity of 20 300 m/s. Open diamonds: slow ions with a velocity of 12 000 m/s. The minimum at 70 fs is an artifact due to interference between the two overlapping laser pulses. Black circles: data on the time dependence of scattered light from a roughened surface (due to material removal), from Ref. 20, shown for comparison.

attribute to Coulomb explosion from the surface are very strongly directed along the surface normal. This is an essential but not necessarily conclusive criterion for the Coulomb-explosion mechanism. The data can be fitted with $\cos^n\theta$ distributions with n on the order of 10. As the velocity distributions shift to lower values and approach the conditions of equal kinetic energy, the angular distributions become considerably broadened, approaching $n<3$ for large numbers of laser shots. The broadening of the angular distribution as more material is removed from the surface is a strong indication that the peaked angular distribution during the gentle phase is not due primarily to hydrodynamical effects in the ablated plume, which can lead to strongly peaked distributions for nanosecond laser ablation.[33] The situation is more complicated for intermediate numbers of laser shots where there are contributions from both gentle and strong ablation. We can also not rule out the influence of crater formation that may be conducive to thermalization of the ion energies. For $N>70$ the depth of the crater becomes comparable to the lateral dimensions of the irradiated region.

Further indications of the mechanisms involved and the relevant time scales for energy coupling are available from time-resolved studies. Figure 7 shows the results of such experiments on Al_2O_3 where two laser pulses (of 0.1 ps duration) of equal fluence (below the ablation threshold) were used to irradiate the same surface spot with a variable delay between the pulses. The sum of the pulse fluences was chosen to lie above the ablation threshold (3.5 J/cm^2). A new spot on the surface was chosen for each delay. The first shot on the surface did not produce any observable ablation. The ion signal was recorded for the double-pulse irradiation as a function of the delay between the two pulses and for two different ion velocities. The results for the Al^+ ions are shown on Fig. 7. The ion velocities were 20 300 m/s (black squares), corresponding to a velocity close to the maximum in the fast, Coulomb-explosion ion distribution for these low

fluences and 12 000 m/s, corresponding to velocities of the slow, thermal ions (open diamonds). For these experiments the TOF axis was normal to the surface so that the velocity maxima are slightly shifted with respect to those shown in Fig. 2 for 25° TOF. For comparison we also show earlier results on the intensity of the scattered light signal as a function of delay time (black circles). This data were taken with a strong first pulse (10 J/cm^2) to initiate ablation and the time scale for bulk material removal was probed by the light scattered from the second, weaker pulse as a function of delay time.[21]

For delay times below 100 fs (the pulse duration) there are strong interference effects between the two overlapping laser pulses. This is the reason for the minimum at a delay of 70 fs. Fast, Coulomb-explosion ions are observed at low delay times up to ~1 ps. In our experiments, the second pulse supplies additional charge density so that the electrostatic stress overcomes the binding energy of the lattice leading to the observed macroscopic Coulomb explosion. The combined charge density decreases after a delay of about 1 ps due to the decrease in charge density that has survived after the first laser pulse. We believe that the dip at 1 ps indicates the time scale for which the charge distribution at the surface initiated by the first laser pulse can remain stable. It decays after ~1 ps due to effects such as, e.g., individual (i.e., not bulk ablation) ion ejection from the surface, hole diffusion from the irradiated area, or electron supply from the bulk or recombination with already ejected electrons. Additionally, and perhaps more importantly, the residual excited electrons in the surface region will decay via electron-phonon coupling on the picosecond time scale. This leads to heating of the lattice and also reduces the efficiency of the surface ionization induced by the second pulse. The slower, thermal ions (open diamonds) start to be observed after a delay of about 1 ps, increasing to a maximum at 10 ps due to the transfer of electronic energy to lattice heating. The signal of fast ions that also rises again and is observed up to 200-ps delay is thought to be due to the high-temperature tail of the thermal ion distribution (Fig. 2) and to have a different origin from the signal that starts to decay at about 1 ps. For delay times beyond about 1 ps the second pulse thus cannot induce sufficient charge density to lead to macroscopic Coulomb explosion but the additional energy input will be used predominantly for heating the lattice. The time scale for the additional heating due to the second laser pulse will also be 1–10 ps. In contrast to the very fast removal of the surface ions due to Coulomb explosion the thermal removal of the bulk material will thus take longer. This is nicely supported by the time behavior of the scattered light, which indicates when the bulk of the material leaves the surface.[21] Our pump-probe ion signal is indicating that the maximum lattice temperature is reached after 10 ps.

This is in very good agreement with the scattered light signal that indicates the onset of the bulk thermal material removal after about 10 ps. The decay of the thermal ion signal for delay times beyond about 100 ps can have two origins. Petite and co-workers have shown that electrons can be trapped either in or close below the conduction band on a time scale of about 100 ps.[34] A more efficient low-order excitation can occur from these excited states than from the higher-order excitation of electrons in the valence band. When these states decay, the energy coupling from the second laser pulse is less efficient and can no longer lead to significant ion removal. Second, and perhaps more importantly for the 100-ps time scale, thermal diffusion will become significant, thus reducing the total thermal excitation in the irradiated area induced by the first laser pulse.

IV. CONCLUSIONS

The results presented in this paper clearly show the occurrence of Coulomb explosion from a highly charged dielectric surface, induced by ultrashort pulse laser irradiation. This is shown by the equal momenta of the positive ions that correspond to impulsive acceleration from a surface with average fractional charge of ~0.65. After a certain incubation period (related to the buildup of defects in the target material) the ablation behavior changes with the maxima in the ion distributions, moving to lower velocities and a broadening of the angular distribution. For a large number of laser shots ($N=100$) the ions have equal kinetic energies. We show that ultrashort pulse laser experiments of the kind demonstrated here, where there is no complication due to the interaction of the laser pulse with emitted material, have considerable potential for aiding our understanding of the conditions under which Coulomb explosion from materials can occur and of the complex behavior of material under extreme conditions.

*Also at: Laser Department, National Institute for Laser, Plasma and Radiation Physics, P.O. Box MG-36, R-76900 Bucharest, Romania.

†Author to whom correspondence should be addressed. FAX: +46 31 772 3496. Email address: f3aec@fy.chalmers.se

[1] *Nanometric Phenomena Induced by Laser, Ion, and Cluster Beams*, special issue of Nucl. Instrum. Methods Phys. Res. B **122**, (1997), edited by E. E. B. Campbell, R. Kelly, G. Marletta, and M. Toulemonde.

[2] D. Bäuerle, *Laser Processing and Chemistry* (Springer, Berlin, 1996).

[3] E. E. B. Campbell, D. Ashkenasi, and A. Rosenfeld, *Lasers in Materials Science* (Trans Tech, Zurich, Switzerland, 1999).

[4] L. S. Bitenskii, M. N. Murakhmetov, and E. S. Parilis, Zh. Tekh. Fiz. **24** (1979) [Sov. Phys. Tech. Phys. **24**, 618 (1979)].

[5] D. H. G. Schneider and M. A. Briere, Phys. Scr. **53**, 228 (1996).

[6] H.-P. Cheng and J. D. Gillaspy, Phys. Rev. B **55**, 2628 (1997).

[7] P. Varga, T. Neidhart, M. Sporn, G. Libiseller, M. Schmid, F. Aumayr, and H. P. Winter, Phys. Scr. **T73**, 307 (1997).

[8] R. E. Marrs, Phys. Scr. **T73**, 354 (1997).

[9] F. Aumayr, J. Burgdörfer, P. Varga, and H.-P. Winter, Comments At. Mol. Phys. **34**, 201 (1999).

[10] J. Limburg, J. Das, S. Schippers, R. Hoekstra, and R. Morgenstern, Phys. Rev. Lett. **73**, 786 (1994).

[11] I. Hughes, Phys. World **8**, 43 (1995).

[12] N. Itabashi, K. Mochiji, H. Shimizu, S. Ohtani, Y. Kato, H. Tanuma, and N. Kobayashi, Jpn. J. Appl. Phys., Part 1 **34**, 6861 (1995).

[13] R. F. W. Herrmann, J. Gerlach, and E. E. B. Campbell, Nucl. Instrum. Methods Phys. Res. B **122**, 401 (1997).

[14] R. Herrmann, J. Gerlach, and E. E. B. Campbell, Appl. Phys. A: Mater. Sci. Process **66**, 35 (1998).
[15] J. Kanasaki, K. Iwata, and K. Tanimura, Phys. Rev. Lett. **82**, 644 (1999).
[16] M. L. Knotek and P. J. Feibelman, Phys. Rev. Lett. **40**, 964 (1978).
[17] H. Varel, M. Wähmer, A. Rosenfeld, D. Ashkenasi, and E. E. B. Campbell, Appl. Surf. Sci. **127-129**, 128 (1998).
[18] D. Ashkenasi, A. Rosenfeld, H. Varel, M. Wähmer, and E. E. B. Campbell, Appl. Surf. Sci. **120**, 65 (1997).
[19] A. C. Tam, J. L. Brand, D. C. Cheng, and W. Zapka, Appl. Phys. Lett. **55**, 2045 (1989).
[20] J. L. Brand and A. C. Tam, Appl. Phys. Lett. **56**, 883 (1990).
[21] A. Rosenfeld, D. Ashkenasi, H. Varel, M. Wähmer, and E. E. B. Campbell, Appl. Surf. Sci. **127-129**, 76 (1998).
[22] R. Haglund and N. Itoh, in *Physics and Applications of Laser Ablation*, edited by J. C. Miller, Springer Series in Materials Science, Vol. 28 (Springer, Heidelberg, 1994), p. 11.
[23] R. Stoian, H. Varel, A. Rosenfeld, D. Ashkenasi, and E. E. B. Campbell, Appl. Surf. Sci. **165**, 44 (2000).
[24] J. S. Pearlman and G. H. Dahlbacka, Appl. Phys. Lett. **31**, 414 (1977).
[25] R. L. Fleischer, P. B. Price, and R. M. Walker, J. Appl. Phys. **36**, 3645 (1965).
[26] M. Polanyi, Z. Phys. **7**, 323 (1921).
[27] D. Ashkenasi, A. Rosenfeld, and R. Stoian (unpublished).
[28] D. Ashkenasi, R. Stoian, and A. Rosenfeld, Appl. Surf. Sci. **154–155**, 40 (2000).
[29] H. Varel, D. Ashkenasi, A. Rosenfeld, R. Herrmann, F. Noack, and E. E. B. Campbell, Appl. Phys. A: Mater. Sci. Process. **62**, 293 (1996).
[30] A.-C. Tien, S. Backus, H. Kapteyn, M. Murnane, and G. Mourou, Phys. Rev. Lett. **82**, 3883 (1999).
[31] R. Kelly and A. Miotello, Nucl. Instrum. Methods Phys. Res. B **122**, 374 (1997).
[32] R. Stoian, D. Ashkenasi, A. Rosenfeld, M. Wittmann, R. Kelly, and E. E. B. Campbell, Nucl. Instrum. Methods Phys. Res. B **166-167**, 682 (2000).
[33] R. Kelly, J. Chem. Phys. **92**, 5047 (1989).
[34] G. Petite, P. Daguzan, S. Guizard, and P. Martin, Nucl. Instrum. Methods Phys. Res. B **107**, 97 (1996).